



Synthesis of lithium nickel cobalt manganese oxide cathode materials by infrared induction heating

Chien-Te Hsieh*, Yu-Fu Chen, Chun-Ting Pai, Chung-Yu Mo

Department of Chemical Engineering and Materials Science, Yuan Ze University, Taoyuan 320, Taiwan



HIGHLIGHTS

- An infrared sintering is adopted to synthesize $\text{LiNi}_{1/3}\text{Co}_{1/3}\text{Mn}_{1/3}\text{O}_2$ (LNCM) powders.
- Crystalline LNCM powders are rapidly synthesized by the induction sintering method.
- The carbon coating onto LNCM is a crucial factor in facilitating cell performance.
- The C-coated LNCM cathode shows high capacity retention at 1C after 50 cycles.

ARTICLE INFO

Article history:

Received 13 March 2014

Received in revised form

4 June 2014

Accepted 24 June 2014

Available online 7 July 2014

Keywords:

Lithium nickel cobalt manganese oxide

Infrared heating

Carbon coating

Lithium ion battery

Cathode materials

ABSTRACT

This study adopts an *in-situ* infrared (IR) sintering incorporated with carbonization technique to synthesize carbon-coated $\text{LiNi}_{1/3}\text{Co}_{1/3}\text{Mn}_{1/3}\text{O}_2$ (LNCM) cathode materials for Li-ion batteries. Compared with electric resistance heating, the *in-situ* IR sintering is capable of rapidly producing highly-crystalline LNCM powders at 900 °C within a short period, i.e., 3 h in this case. Glucose additive is employed to serve a carbon precursor, which is carbonized and coated over the surface of LNCM crystals during the IR sintering process. The electrochemical performance of LNCM cathodes is well examined by charge-discharge cycling at 0.1–5C. An appropriate carbon coating is capable of raising discharge capacity (i.e., 181.5 mAh g⁻¹ at 0.1C), rate capability (i.e., 75.0 mAh g⁻¹ at 5C), and cycling stability (i.e., capacity retention: 94.2% at 1C after 50 cycles) of LNCM cathodes. This enhanced performance can be ascribed to the carbon coating onto the external surface of LNCM powders, creating an outer circuit of charge-transfer pathway and preventing cathode corrosion from direct contact to the electrolyte. Accordingly, the *in-situ* IR sintering technique offers a potential feasibility for synthesizing cathode materials commercially in large scale.

© 2014 Elsevier B.V. All rights reserved.

1. Introduction

Lithium-ion battery is one of the most preferred power sources for portable electronic devices due to its high gravimetric and volumetric energy densities [1,2]. Up to now, one layered alkali transition metal oxide, LiCoO_2 , has been in wide use as cathode materials, owing to its stability and high rate capability [3–5]. For example, Y.P. Fu group developed sol-gel technique to synthesize high-performance LiCoO_2 cathode materials [6]. They also used facile chemical method to prepare C-coated LiCoO_2 cathode in 2007 [7]. However, there is increasing demand for alternative materials to commercial LiCoO_2 . The most challenging factor for LiCoO_2 cathode material is its expensive price because of the use of costly

cobalt precursor. In order to reduce costly Co content, one multi-elemental cathode, $\text{LiNi}_{1/3}\text{Co}_{1/3}\text{Mn}_{1/3}\text{O}_2$ (LNCM), has received considerable attentions because of its high specific capacity, superior thermal stability, and lower Co-content making it more effective and less toxic [8,9]. Accordingly, pioneering studies have reported reliable synthesis of LNCM such as polymer template route [2], mixed hydroxide method [3], array transfer method [4], inverse micro-emulsion route [9], sol-gel method [8,10,11] and co-precipitation method [5,12]. More recently, our previous study also developed a chemical-wet synthesis incorporated with pulse microwave-assisted heating precursors and carbon coating technique to prepare highly-crystalline LNCM powders [13]. The LNCM cathodes are observed to show superior electrochemical performance, e.g., high specific capacity and cyclic stability. In traditional furnaces equipped with electric resistance heating systems, the sintering process is run at high temperatures between 600 and 900 °C, while make highly-crystalline LNCM grains. The sintering

* Corresponding author. Tel.: +886 3 4638800x2577; fax: +886 3 4559373.

E-mail address: cthsieh@saturn.yzu.edu.tw (C.-T. Hsieh).

process usually takes a long heating period, ranging from 6–22 h. This drawback would cause higher electricity consumption and thus raise the production cost, which is not suitable for mass production.

To resolve the above problem, one strategy proposed here is to look for a low-cost synthesis method with short heating period. Recently, S. Uchida et al. employed a high-frequency induction heating incorporated with carbothermal reduction to synthesize C/LiFePO₄ composite in vacuum [14]. The induction heating technique allows the fast formation of olivine cathodes, opening a possibility to prepare cathode materials rapidly by induction heating. Herein the present work aims at fast synthesis of LNCM cathode using an induction heating infrared (IR) source. In fact, IR heating has been used extensively for surface coating, drying and curing of paints and coatings, moisture removal, and many practical applications [15]. Some researchers adopted the IR heating technique to sinter NiO buffer layer [16] and Ag nanoparticles on paper [17]. It is generally recognized that IR ray is an electromagnetic radiation with wavelength between visible light and microwave radiation [18]. Compared with traditional convective heating, the advantages of IR heater consist of (i) fast adsorber heat-up times, (ii) ability for programmable heating, (iii) controllability and (iv) high energy efficiency [15,19]. Besides, carbon coating is a crucial technique to

improve the poor cyclic stability of LNCM cathodes, resulting from its low electronic conductivity, high reactivity between delithiated cathode and electrolyte, and serious dissolution of transition metal ions and electrolyte [20–22]. Hence, this study proposes an *in-situ* IR sintering combined with carbonization process to synthesize C/LNCM composites in a home-made induction oven, equipped with an IR heater array. Herein four LNCM cathodes with different carbon contents have been synthesized to explore their electrochemical performance, using charge–discharge measurement.

2. Experimental

The *in-situ* IR sintering incorporated with carbonization method was described as follows. First, the LNCM precursors, consisted of CH₃COOLi·2H₂O ($\geq 99.0\%$), Ni(CH₃COO)₂·4H₂O ($\geq 98.0\%$), Co(CH₃COO)₂·4H₂O ($\geq 99.5\%$), and Mn(CH₃COO)₂·4H₂O ($\geq 99.0\%$), were dissolved in distilled water in a baker, forming a brownish metallic slurry. The stoichiometric ratio of metal ion solution was fixed at 3.3:1:1:1 in Li:Ni:Co:Mn, respectively. Here glucose (C₆H₁₂O₆) was chosen as carbon source, and the weight percentages of glucose in the LNCM precursors were set at 0.1, 0.25, 0.5, and 0.75%. The glucose solution was slowly added into the metallic slurry and then

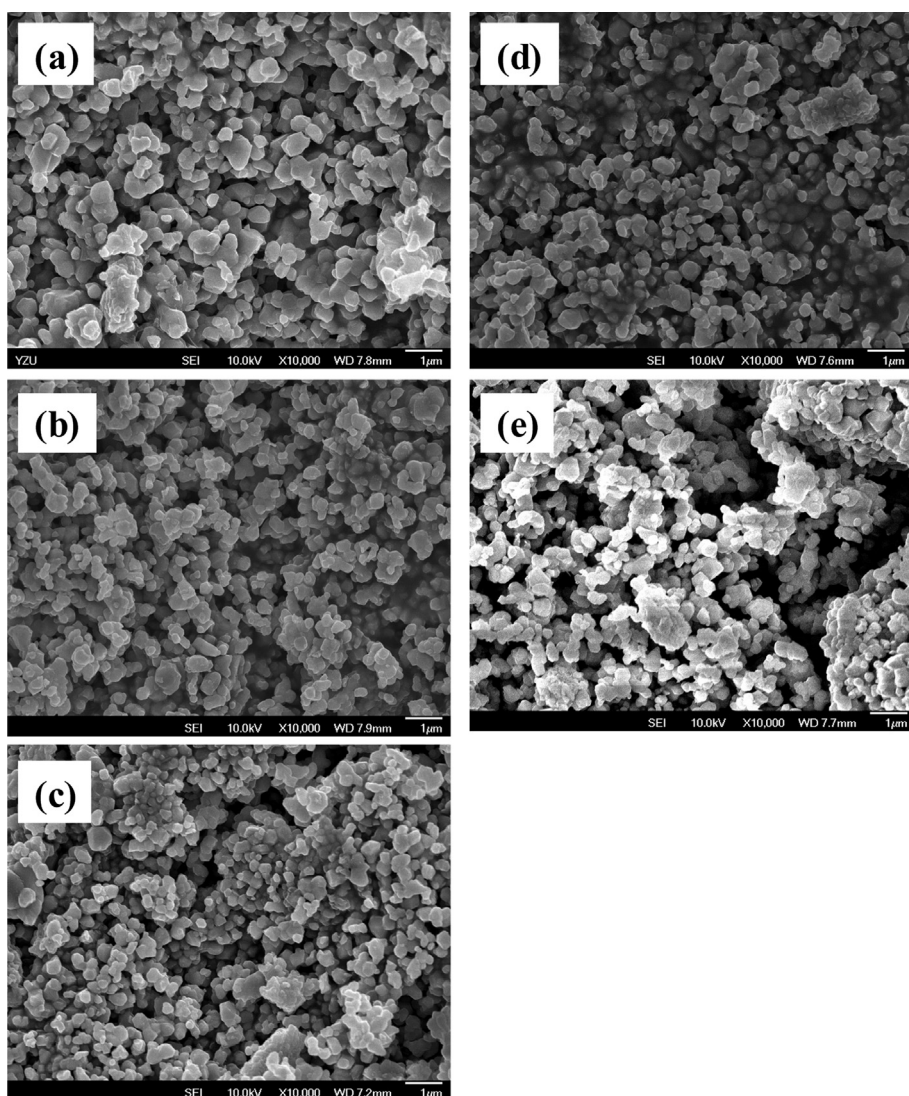


Fig. 1. FE-SEM images of (a) fresh LNCM, (b) LNCM-C1, (c) LNCM-C2, (d) LNCM-C3, and (e) LNCM-C4 powders.

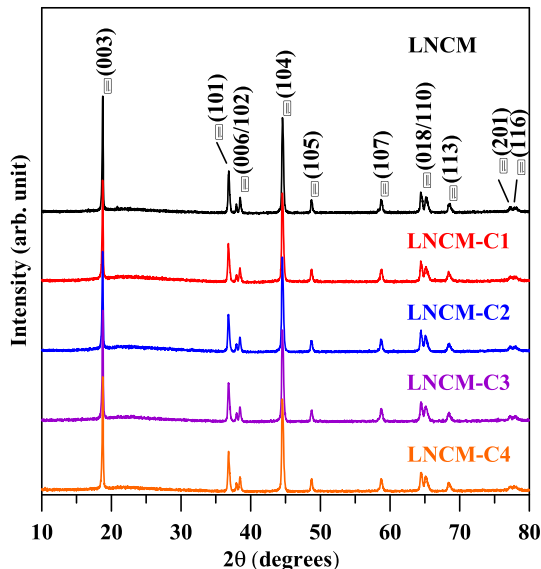


Fig. 2. Typical XRD patterns for fresh LNCM and C/LNCM powders prepared from the *in-situ* IR sintering technique.

homogeneously mixed using a high-performance homogenizer for 1 h. After that, the baker was placed into a vacuum oven and heated at 120 °C for 6 h, ensuring the removal of moisture. The dried precursor powders were put into a home-made IR induction oven, which is equipped with six carbon fiber (CF) heaters. The CF heaters, with a near-IR wavelength region of 1–5 μm, are capable of transferring energy to a body through electromagnetic radiation. Thus, no contact or medium between the two bodies was needed for the energy transfer. A two-step heat treatment was used to prepare the C/LNCM composites in the closed IR induction oven, composed of (i) preheat-treatment and (ii) IR sintering combined with carbonization. The preheat-treatment of LNCM precursor was performed at 350 °C with a heating rate of

80 °C min⁻¹ and kept at this temperature for 1 h. The *in-situ* IR sintering was then carried out in the IR induction oven at 900 °C in inert atmosphere (N₂) for 3 h. At last, the final C/LNCM products were naturally cooled in the IR induction oven. The C/LNCM powders were designated to LNCM-C1, LNCM-C2, LNCM-C3, and LNCM-C4, according to different amounts of glucose of 0.1, 0.25, 0.5, and 0.75%, respectively.

Field-emission scanning electron microscope (FE-SEM, JEOL JSM-5600) and high-resolution transmission electron microscope (HR-TEM, JEOL, JEM-2100) were adopted to observe the microstructures of C/LNCM powders. The HR-TEM observation was carried out using a microscope operating at 200 kV. An X-ray diffraction (XRD, Shimadzu Labx XRD-6000) spectrometer, equipped with Cu-Kα radiation emitter, was used to analyze the crystalline structures of the LNCM samples.

The electrochemical performance of C/LNCM cathode materials was examined by using CR2032-type coin cells. As for the cell assembly, the C/LNCM cathode powders were mixed with two conducting media (Super-P and KS-4) and one binder (polyvinylidenefluoride, PVDF). The weight ratio of C/LNCM: PVDF: Super-P: KS-4 was set at 80:10:5:5. One organic solvent, *N*-methyl pyrrolidinone (NMP), was then poured into the solid mixture to form the electrode slurry. The slurry was uniformly blended by a three-dimensional mixer using Zr balls for 3 h, and the resultant slurry was pasted on an Al foil substrate with a doctor blade, followed by evaporating NMP with a blow dryer. The prepared C/LNCM cathode sheets were dried at 135 °C in a vacuum oven for 12 h. Then the electrode sheets were pressed under a pressure of approximately 200 kg cm⁻², and the electrode layers were adjusted to a thickness of ca. 100 μm. After that, the CR2032 coin cells were assembled in a glove box. Herein the Li foil and the porous polypropylene film were used as the counter electrode and the separator, respectively. The electrolyte solution was 1.0 M LiPF₆ in a mixture of ethylene carbonate, polycarbonate, and dimethyl carbonate with a weight ratio of 1:1:1. The charge/discharge cycling tests at different C rates (from 0.1 to 5C) were carried out within the potential range between 2.8 and 4.5 V vs. Li/Li⁺ at ambient temperature.

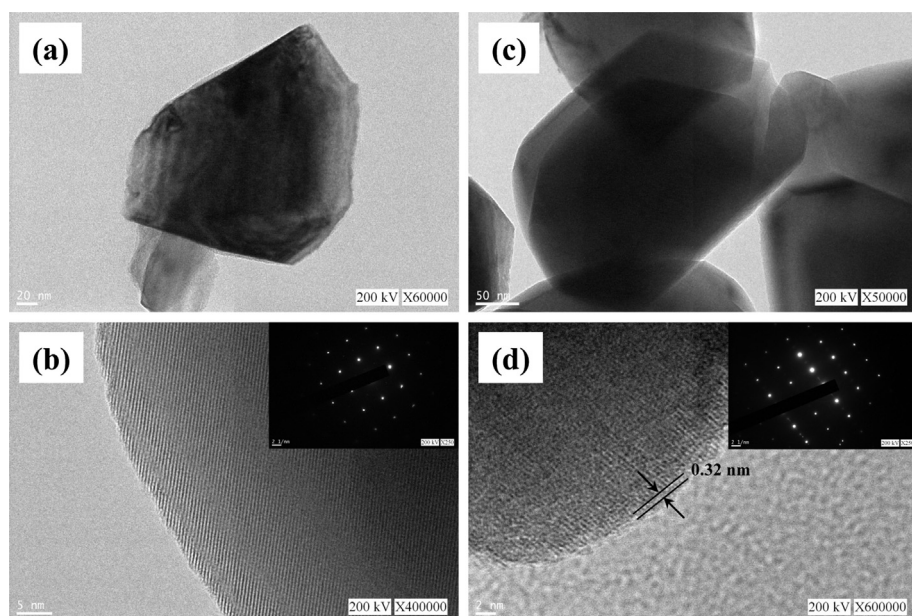


Fig. 3. (a) HR-TEM micrograph and (b) lattice fringes of fresh LNCM powder. (c) HR-TEM micrograph and (d) lattice fringes of fresh LNCM-C1 powder. The insets of (b) and (d) show SAED patterns of fresh LNCM and LNCM-C1 crystals, respectively.

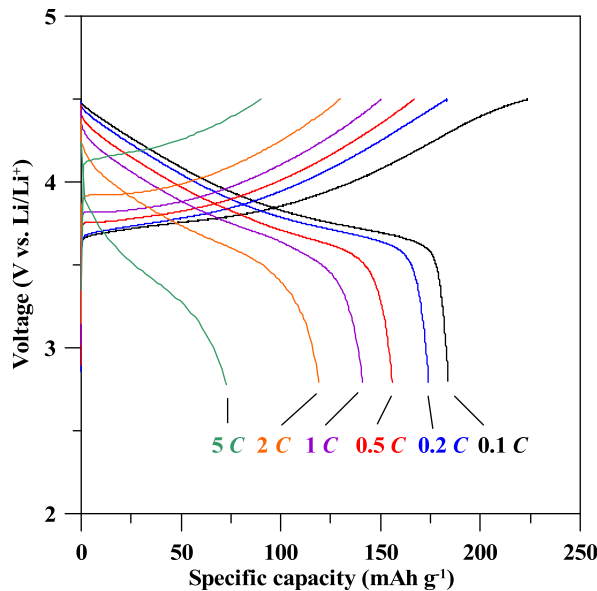


Fig. 4. Typical charge/discharge curves of fresh LNCM cathode at different C rates.

3. Results and discussion

Fig. 1(a)–(e) illustrate top-view FE-SEM photographs of fresh LNCM and C/LNCM powders through the *in-situ* IR induction heating at 900 °C. The polyhedral-shaped LNCM powders basically appear as a homogeneous dispersion with slight aggregation. The mean particle size of all LNCM particles is approximately 500 nm. Accordingly, the influence of carbon coating on the particle size and dispersion of C/LNCM powders seems to be minor. Energy diffraction spectroscopy (EDS) analysis was adopted to examine the atomic ratio of C in the LNCM powders. The result reveals that these C/LNCM particles contain carbon contents as the following order: LNCM-C1 (0.08 wt%) < LNCM-C2 (0.12 wt%) < LNCM-C3 (0.27 wt%) < LNCM-C4 (0.38 wt%), identical to the sequence of glucose amount.

Fig. 2 shows typical XRD patterns of fresh LNCM and C/LNCM powders, indicating the presence of α -NaFeO₂ crystal structure with a space group of rhombohedral $R\bar{3}m$ symmetry [23]. The diffraction peaks of LNCM crystals are well defined, and the lattice parameters of fresh LNCM samples can be calculated as $a = 2.860 \text{ \AA}$ and $c = 14.134 \text{ \AA}$. After the carbon coating, the C/LNCM composites show very slight deviations from the lattice parameters, where $a = 2.863\text{--}2.865 \text{ \AA}$ and $c = 14.179\text{--}14.194 \text{ \AA}$. It is worth noting that the splitting of hexagonal doublets (006)/(012) and (108)/(110) takes place at 38° and 65°, respectively. This finding confirms the presence of highly-ordered layer structure of LNCM [8,23]. In addition, one R ratio, defined by the peak intensity ratio of (003) to (104) lines, can serve as an important factor in determining the degree of cation mixing. Generally, a smaller R ratio represents a higher degree of disorder cation mixing. The fresh LNCM sample possesses a high R ratio of 1.335, whereas the R ratio of C/LNCM composites ranges from 1.056 to 1.232. This slight decrease in the R ratio is presumably due to the carbon mixing that partially distributes atomic arrangement of LNCM crystals.

Fig. 3(a) and (b) shows HR-TEM micrographs of fresh LNCM powder, confirming the polyhedral-shaped particle with well-defined lattice fringes. As observed from Fig. 3(b), the interspacing distance is approximately 4.72 Å, assigned to the (003) planes [23]. Fig. 3(c) and (d) depicts HR-TEM micrographs of LNCM-C1 sample, indicating that the LNCM particles basically display a

polyhedral shape after the carbon coating. The observation is in agreement with FE-SEM analysis. It is observed that a carbon layer with an average thickness of 0.32 nm is coated over the surface of LNCM powder. The formation of carbon layer can be attributed to the fact that the carbonization of glucose under IR irradiation is prone to deposit amorphous carbon layer onto the LNCM powders at 900 °C. A selected-area diffraction (SAD) was used to analyze the crystalline LNCM grain, as shown in the inset of Fig. 3(b) and (d). For comparison, both SAD images reflect regular spot arrays that can be assigned to single crystalline pattern of α -NaFeO₂ crystal structure with $R\bar{3}m$ symmetry [13].

On the basis of the results, the *in-situ* IR sintering incorporated with carbonization method is capable of creating highly-crystalline LNCM powders within a shorter period, as compared with the traditional contact heating. It is well known that IR heat is radiation that is a simple form of energy without direct energy losses to visible and ultraviolet light [18]. In this study, the CF heater arrays emit electromagnetic radiation, generating a surrounding with uniform temperature distribution. The LNCM precursors can adsorb the radiation heat at initial stage, followed by convective heat transfer from the CF heater to the surface of LNCM mixture. Thus, the induction heating rapidly raises the inner temperature in the solid mixture, reaching the crystallization temperature of LNCM grains. Meanwhile, the glucose additive is decomposed into C content at carbonization temperature of 600–900 °C and then coated over the surface of LNCM grains. As a result, the *in-situ* IR sintering allows two reaction pathways: (i) formation of LNCM grains and (ii) creation of carbon layer, inducing C/LNCM composites. Since the induction heating enables the fast synthesis of LNCM crystals, the *in-situ* IR sintering technique displays a potential feasibility to prepare highly-crystalline cathode materials with large-scale production, based on the unique CF heater arrays.

Typical charge–discharge curves of fresh LNCM electrodes between 2.8 and 4.5 V at different C rates are illustrated in Fig. 4. The fresh LNCM cathode exhibits an initial discharge capacity of ca. 175.2 mAh g⁻¹ at 0.1C. At 5C, the cathode still remains the specific capacity of 75.2 mAh g⁻¹, showing a possibility for high-power applications. The fast reversible capacity is attributed to the redox couple of $\text{Ni}^{2+}/\text{Ni}^{4+}$ in α -NaFeO₂ nanocrystals. It is generally recognized that Mn⁴⁺ is electrochemically inactive, and the redox of Co^{3+/-4+} takes place at a potential range greater than 4.6 V [24]. The C/LNCM composite cathodes prepared from the *in-situ* IR sintering were subjected to charge–discharge test at different C rates, ranging from 2.8 to 4.5 V, as shown in Fig. 5(a) and (b). The curves clearly indicate that the LNCM-C1 cathode offers the highest discharge capacity of 181.5 mAh g⁻¹ at 0.1C among these C/LNCM cathodes. Among the C/LNCM cathodes, the LNCM-C1 also exhibits the best rate capability at other C rates, e.g., specific capacity: 75.0 mAh g⁻¹ at 5C. As a result, the other three C/LNCM composites cathodes possess high low-rate capacity (i.e., >150 mAh g⁻¹ at 0.1C) but poor rate ability at 5C, as compared with fresh LNCM and LNCM-C1 ones. This result originates from the reason that thick carbon layer is prone to easily bind single LNCM particles and form inter-particle aggregates, reducing low diffusivity of Li ions in the LNCM crystals. Hence, an appropriate amount of carbon content plays the positive effect on the improved discharge capacity and the rate capability of LNCM electrodes.

Fig. 6 shows the cyclic performance of fresh LNCM and C/LNCM cathodes charged and discharged at 1C within the potential range of 2.8–4.5 V. It can be viewed that fresh LNCM cathode displays an obvious capacity decay after the charge–discharge cycling. The capacity retention of fifth to first cycle for all LNCM cathodes can be viewed as LNCM-C2 (97.5%) > LNCM-C1 (94.2%) > LNCM-C3 (92.0%) > LNCM-C4 (81.5%) > fresh LNCM (51.7%). This result reflects the importance of carbon coating over LNCM cathode that

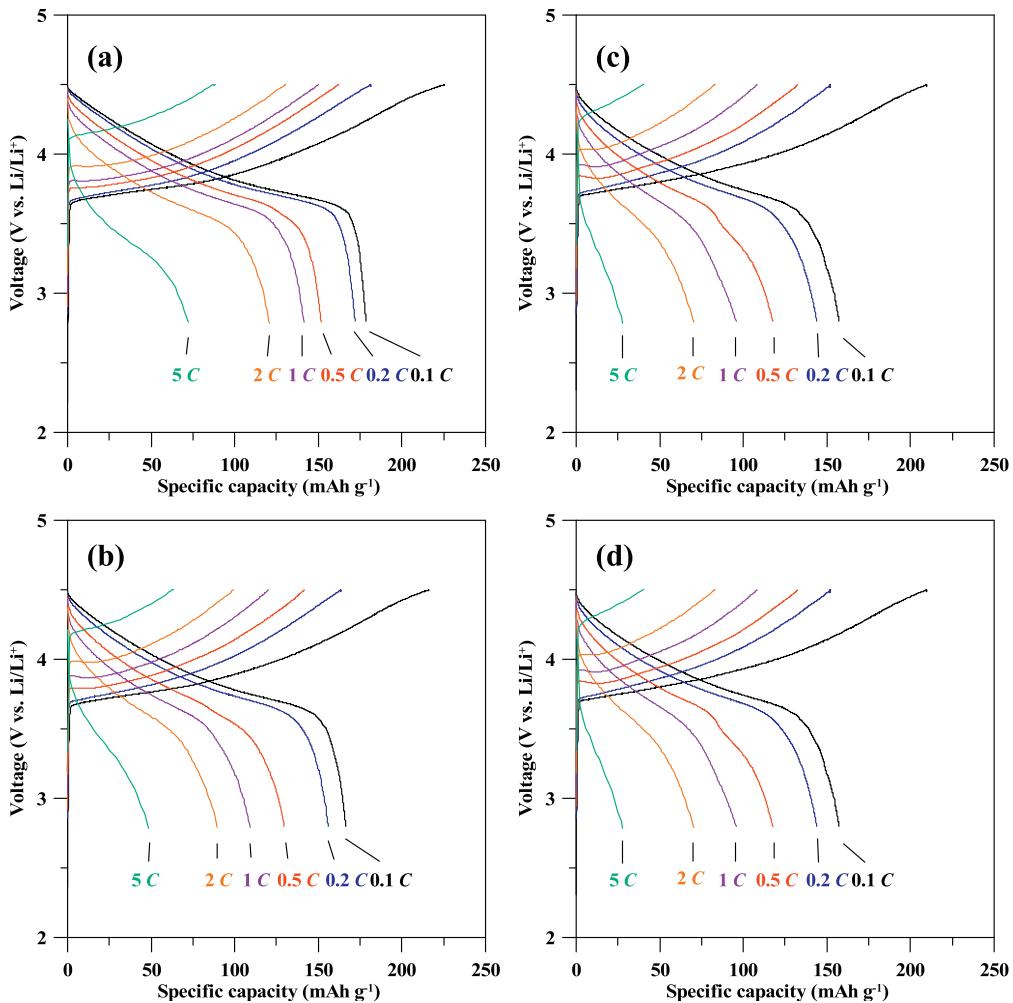


Fig. 5. Typical charge/discharge curves of (a) LNCM-C1, (b) LNCM-C2, (c) LNCM-C3, and (d) LNCM-C4 cathodes at different C rates.

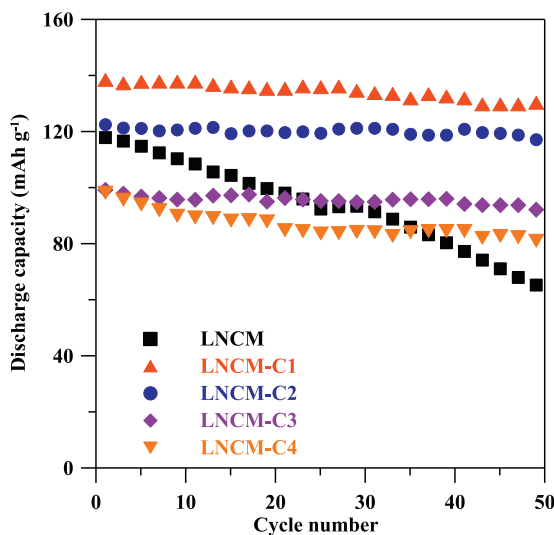


Fig. 6. The cyclic performance of fresh LNCM and C/LNCM cathodes charged and discharged at 1C within the potential range of 2.8–4.5 V.

significantly leads to good reversibility of lithiation/delithiation process at high rates, improving the cyclic performance. Generally, the LNCM cathode suffers from unsatisfied cycling stability due to its low electronic conductivity, high reactivity between delithiated cathode and electrolyte, and serious dissolution of transition metal ions and electrolyte [20]. However, the carbon coating technique could avoid the above situations. The optimal carbon coating (e.g., the LNCM-C1 cathode) onto the surface of LNCM cathode via the *in-situ* IR heating not only protect the dissolution of transition metals but also assist the Li⁺ diffusion in the solid solution and e jumping across the electrode [13]. Based on the viewpoint on the superior performance and fast fabrication, the *in-situ* IR sintering technique opens a possibility to produce high-performance LNCM cathode powders in commercial scale.

4. Conclusions

We have fabricated highly-crystalline LNCM cathode materials using an *in-situ* infrared sintering incorporated with carbonization technique. The *in-situ* IR sintering was adopted to synthesize C/LNCM powders at 900 °C within a shorter period, as compared with traditional electric resistance heating. The carbon coating was uniformly covered the surface of LNCM powders by carbonizing the glucose precursor during the IR sintering process. The

electrochemical performance of LNCM cathodes was well investigated by charge–discharge cycling at 0.1–5C. Among these LNCM cathodes, the LNCM-C1 cathode displayed the best performance, including discharge capacity (i.e., 181.5 mAh g⁻¹ at 0.1C), rate capability (i.e., 75.0 mAh g⁻¹ at 5C), and cycling stability (i.e., capacity retention: 94.2% at 1C after 50 cycles). The improved performance could be ascribed to the fact that the optimal carbon coating (e.g., the LNCM-C1 cathode) onto the surface of LNCM cathode via the *in-situ* IR heating not only protect the dissolution of transition metals but also assist the ionic diffusion in the solid solution and electron jumping across the electrode. On the basis of the experimental results, the *in-situ* IR sintering offered an efficient route to fast synthesize C/LNCM cathodes for high-performance Li-ion battery.

Acknowledgments

The authors are very grateful for the financial support from the National Science Council of Taiwan under the contract NSC 101-2628-E-155-001-MY3.

References

- [1] G.-A. Nazri, G. Pistoia, *Lithium Batteries: Science and Technology*, Kluwer, Boston, 2004.
- [2] N.N. Sinha, N. Munichandraiah, *J. Electrochem. Soc.* 157 (2010) A647–A653.
- [3] S.-C. Yin, Y.-H. Rho, I. Swainson, L.F. Nazar, *Chem. Mater.* 18 (2006) 1901–1910.
- [4] M. Roberts, J. Owen, *ACS Comb. Sci.* 13 (2011) 126–134.
- [5] N. Yabuuchi, Y. Koyama, N. Nakayama, T. Ohzuku, *J. Electrochem. Soc.* 152 (2005) A1434–A1440.
- [6] L.J. Fu, H. Liu, C. Li, Y.P. Wu, E. Rahm, R. Holze, H.Q. Wu, *Prog. Mater. Sci.* 50 (2005) 881–928.
- [7] Q. Cao, H.P. Zhang, G.J. Wang, Q. Xia, Y.P. Wu, H.Q. Wu, *Electrochim. Commun.* 9 (2007) 1228–1232.
- [8] P. Gao, Y. Li, H. Liu, J. Pinto, X. Jiang, G. Yang, *J. Electrochem. Soc.* 159 (2012) A506–A513.
- [9] N.N. Sinha, N. Munichandraiah, *ACS Appl. Mater. Interfaces* 6 (2009) 1241–1249.
- [10] B.J. Hwang, Y.W. Tsai, D. Carlier, G. Ceder, *Chem. Mater.* 15 (2003) 3676–3682.
- [11] J. Zheng, J.-J. Chen, X. Jia, J. Song, C. Wang, M.-S. Zheng, Q.-F. Dong, *J. Electrochem. Soc.* 157 (2010) A702–A706.
- [12] Y.-S. Lee, K.-S. Lee, Y.-K. Sun, Y.M. Lee, D.-W. Kim, *J. Power Sources* 196 (2011) 6997–7001.
- [13] C.-T. Hsieh, C.-Y. Mo, Y.-F. Chen, Y.-J. Chung, *Electrochim. Acta* 106 (2013) 525–533.
- [14] S. Uchida, M. Yamagata, M. Ishikawa, *J. Power Sources* 243 (2013) 481–487.
- [15] M.T. Brogan, P.F. Monaghan, *Compos. Part A* 27 (1996) 301–306.
- [16] J.-K. Chung, W.-J. Kim, J. Tak, C.J. Kim, *Phys. C* 463–465 (2007) 619–624.
- [17] D. Tobjörk, H. Aarnio, P. Pulkkinen, R. Bollström, A. Määttänen, P. Ihälainen, T. Mäkelä, J. Peltonen, M. Toivakka, H. Tenhu, R. Österbacka, *Thin Solid Films* 520 (2012) 2949–2955.
- [18] K. Witek, T. Piotrowski, A. Skwarek, *Mater. Sci. Eng. B* 177 (2012) 1373–1377.
- [19] G.J. Sweeney, P.F. Monaghan, M.T. Brogan, S.F. Cassidy, *Compos. Pt. A Appl. Sci. Manuf.* 6 (1995) 255–262.
- [20] F. Wu, M. Wang, Y. Su, S. Chen, B. Xu, *J. Power Sources* 191 (2009) 628–632.
- [21] M.L. Marciniek, J.W. Wilcox, M.M. Doeff, R.M. Kostecki, *J. Electrochem. Soc.* 156 (2009) A48–A51.
- [22] Z.-D. Huang, B. Zhang, Y.-B. He, S.-W. Oh, Y. Yu, J.-K. Kim, *J. Electrochem. Soc.* 159 (2012) A2024–A2028.
- [23] C.V. Rao, A.L.M. Reddy, Y. Ishikawa, P.M. Ajayan, *ACS Appl. Mater. Interfaces* 3 (2011) 2966–2972.
- [24] K.M. Shaju, G.V.S. Rao, B.V.R. Chowdari, *Electrochim. Acta* 48 (2002) 145–151.